

Nuclear effects in the deuteron in the resonance and
deep-inelastic scattering region

Ядерные эффекты в дейтроне в резонансной и
глубокоупругой областях

S.A. Kulagin^{a,1}

^a Institute for Nuclear Research of the Russian Academy of Sciences
60-letiya Oktyabrya Prosp. 7a, Moscow 117312, Russia

Обсуждается гибридная модель неупругих структурных функций протона и нейтрона, учитывающая как партонные так и резонансные структуры и применимая в широкой области значений масс W рожденных адронных состояний. Для типичной кинематической области экспериментов JLab вычислены структурные функции дейтрона и показано хорошее согласие модельных предсказаний с экспериментальными данными. Модель применяется для систематического исследования отношений F_2^n/F_2^d и $(F_2^p + F_2^n)/F_2^d$ как в глубокоупругой так и в резонансной областях в контексте анализа результатов эксперимента BoNuS в Jefferson Lab.

We discuss a hybrid model of the proton and neutron inelastic structure functions which incorporates both the partonic and the nucleon resonance structures and applicable in a wide region of the invariant mass W of produced hadronic states. Focusing at the typical kinematics of JLab experiments we compute the deuteron structure functions and demonstrate good performance of the model against data. We perform systematic study of the ratios F_2^n/F_2^d and $(F_2^p + F_2^n)/F_2^d$ for both, the deep-inelastic and the resonance, region in the context of recent measurements of BoNuS experiment at Jefferson Lab.

PACS: 25.30.Rw; 13.60.Hb

1. Introduction

The BoNuS experiment at JLab recently reported a precise measurement of the ratio of the neutron and the deuteron structure functions F_2^n/F_2^d covering a wide region of Bjorken x and 4-momentum transfer squared Q^2 between 0.7 and 4.5 GeV² [1]. Those data, in combination with the “world” data on the ratio F_2^p/F_2^d , were used in Ref. [2] in order to extract $R^d = F_2^d/(F_2^p + F_2^n)$ thus providing a measurement of the EMC effect in the deuteron. The purpose of this paper is to compute the deuteron structure function F_2^d and study the ratios R^d and F_2^n/F_2^d in the kinematic region of BoNuS experiment. Note that BoNuS data were taken at relatively low values of the invariant momentum transfer

¹E-mail: kulagin@ms2.inr.ac.ru

Q and also a significant part of data fall into the nucleon resonance region. For this reason in Sec.2 we develop a model of the proton and the neutron structure functions which incorporates both the partonic and the resonance structures and spans a wide region of mass W of produced hadronic states, from inelastic threshold to the deep-inelastic scattering region. In Sec.3 we focus on the computation of the deuteron structure function F_2^d and discuss model predictions for both the deep-inelastic and the resonance regions. We then perform a detailed comparison of our predictions with data of Refs. [1, 2].

2. The proton and the neutron structure functions

For inelastic electron scattering off a proton (neutron) with four-momentum p and four-momentum transfer q , the different scattering regions are commonly characterized by the invariant mass squared of produced hadronic states $W^2 = (p+q)^2 = p^2 + Q^2(1/x - 1)$, where $Q^2 = -q^2$ and $x = Q^2/(2p \cdot q)$ is the dimensionless Bjorken variable. The region of $W > 2$ GeV and $Q > 1$ GeV is referred to as deep-inelastic scattering (DIS), in which the cross section is driven by scattering off quasi-free (anti)quarks in hadrons described by the parton distribution functions (PDFs). The structure functions (SF) depend on two independent variables, usually x and Q^2 . A common framework to describe DIS is the operator product expansion (OPE) which produce the power series in Q^{-2} (twist expansion). In the first order, i.e. in the leading twist (LT), SFs are fully determined by PDFs. The power corrections can be of two different types: (i) contributions from higher-twist (HT) operators describing quark-gluon correlations and (ii) correction arising from a finite nucleon mass (target mass correction, or TMC). We also note that for the sake of computing the deuteron SF (see Sec.3), the nucleon SF are required in off-mass-shell region $p^2 < M^2$, where M is the nucleon mass. Summarizing, the nucleon SF can be written as follows (which we will refer to as the DIS model)

$$F_2^{\text{DIS}}(x, Q^2, p^2) = F_2^{\text{TMC}}(x, Q^2, p^2) + H_2(x)/Q^2, \quad (1)$$

where F_2^{TMC} is the LT SF corrected for the target mass effects and H_2 describes the dynamical twist-4 contribution (for brevity, we suppress explicit notation to the twists higher than 4). In this paper the LT SF is computed using the proton and the neutron PDFs from a global PDF fit of Ref. [3, 4]. We note that the studies of Ref. [3, 4] were performed to the next-to-next-to-leading-order (NNLO) approximation in QCD coupling constant with a special emphasis on a low- Q region and constrain the nucleon SF, including the HT terms, for $Q^2 \geq 1$ GeV².

In order to account for TMC, we follow Ref. [5]. Since the calculation of nuclear SF requires the nucleon SF in off-mass-shell region, we analytically continue the equations of Ref. [5] in the off-shell region by replacing the nucleon mass squared M^2 with p^2 . In particular, for F_2 we have

$$F_2^{\text{TMC}}(x, Q^2, p^2) = \frac{x^2}{\xi^2 \gamma^3} F_2^{\text{LT}}(\xi, Q^2, p^2) + \frac{6x^3 p^2}{Q^2 \gamma^4} \int_{\xi}^1 \frac{d\xi'}{\xi'^2} \left[1 + \frac{2xp^2}{\gamma Q^2} (\xi' - \xi) \right] F_2^{\text{LT}}(\xi', Q^2, p^2), \quad (2)$$

where $\xi = 2x/(1 + \gamma)$ is the Nachtmann variable and $\gamma = (1 + 4x^2 p^2/Q^2)^{1/2}$.

It should be noted, that TMC procedure of Ref. [5] violates the $x \rightarrow 1$ behavior leading to nonzero F_2 at and below the inelastic threshold (see, e.g., discussion in [6]). The region of large Bjorken $x \sim 1$ corresponds to low W and is affected by excitations of the nucleon resonances. Clearly this is outside of the partonic picture of DIS. In order to suppress contributions from low W and formally obey the inelastic threshold requirement, we multiply F_2^{DIS} by the function $f_{\text{th}}(W) = 1 - \exp[(W_{\text{th}} - W)/d]$, where $W_{\text{th}} = M + m_\pi$ with m_π the pion mass. We also assume that the parameter d is of order of the pion mass and use $d = 0.15$ GeV in the analysis discussed below. This will ensure vanishing F_2 at the inelastic threshold $W = W_{\text{th}}$, and we also have $f_{\text{th}} = 1$ with a high accuracy for the W values above the resonance region (at practice this also holds for the second and the third resonance region).

In off-mass-shell region the structure function explicitly depends on the nucleon invariant mass squared p^2 . This dependence has two different sources: (i) the terms p^2/Q^2 in Eq.(2) which lead to power terms at large values of Q^2 and (ii) nonpower terms from off-shell dependence of the LT SF. Following Ref. [6, 7] we observe that for computing the nuclear SF it would be enough to know the proton and the neutron SF in the vicinity of the mass shell $p^2 = M^2$. Then we use the nucleon virtuality $v = (p^2 - M^2)/M^2$ as a small parameter and expand the SF in series in v . To the leading order in v we have

$$F_2^{\text{LT}}(x, Q^2, p^2) = F_2^{\text{LT}}(x, Q^2) [1 + \delta f(x, Q^2) v], \quad (3)$$

$$\delta f(x, Q^2) = M^2 \partial_{p^2} \ln F_2^{\text{LT}}(x, Q^2, p^2), \quad (4)$$

where F_2^{LT} on the right-hand side in Eq.(3) is the structure function of the on-mass-shell nucleon and ∂_{p^2} in Eq.(4) denotes the partial derivative with respect to p^2 taken on the mass shell $p^2 = M^2$. The function δf describes the relative modification of the nucleon SF and PDFs in the vicinity of the mass shell. A detailed study of nuclear DIS and Drell-Yan process in Refs. [6, 8, 9] and also recent global PDF analysis in Ref. [10] indicate no significant Q^2 as well as the nucleon isospin dependence of δf . Following these observations we assume the function Eq.(4) to be Q^2 independent and identical for the proton and the neutron, i.e. $\delta f^{p,n}(x, Q^2) = \delta f(x)$.

The region $W < 2$ GeV is driven by excitation of nucleon resonances which show up as pronounced structures in the cross-sections. We first consider the proton SF. In order to model the proton SF in this region, we use the results of empirical fit of Ref. [11], which takes into account the contribution from a few resonances as well as nonresonance background:

$$F_2^{\text{RES}}(x, Q^2, p^2) = F_2^{\text{CB}}(Q^2, W^2). \quad (5)$$

The SF computed by Eq.(5) will be referred to as the RES model. It should be noted that in the overlap region, in particular for $1.8 < W < 3$ GeV and $1 < Q^2 < 9$ GeV², the results of the DIS [3, 4] and the RES [11] fits are in a nice correspondence motivating us to use a combined DIS-RES model, which spans a wide region of W . For a combined SF model we will use the DIS model (1) for $W > W_2 = 2$ GeV and the RES model (5) for $W < W_1 = 1.8$ GeV. In order to insure the continuity of the resulting function, we interpolate between the DIS and the RES models within the region $W_1 < W < W_2$ using a linear in W function (the details of this model will be discussed elsewhere).

It is worth mentioning that on average the DIS and the RES model give nearly equivalent description in the resonance region (the quark-hadron duality phenomenon [12],

for a review see Ref. [13]). In particular, for the integral over the region from the inelastic threshold $W_{\text{th}} = M + m_\pi$ to $W = W_2$ we find that the relation

$$\int_{W_{\text{th}}^2}^{W_2^2} dW^2 F_2^{p(\text{DIS})}(x, Q^2) = \int_{W_{\text{th}}^2}^{W_2^2} dW^2 F_2^{p(\text{RES})}(x, Q^2) \quad (6)$$

holds with a good accuracy in the region $1 < Q^2 < 9 \text{ GeV}^2$ with a maximum difference between the DIS and the RES integral about 5%.

Note that the discussion above refers to the proton and now we consider the model of the neutron SF. In the DIS region, the neutron LT SF is computed in terms of the proton PDFs relying on the isospin symmetry. The isospin relations for the HT terms are not so obvious. However, the isospin effect on the HT contribution was constrained phenomenologically from a global QCD analysis using proton and deuteron DIS data [4, 10, 14] and we use these results in order to compute the neutron SF. In the resonance region, an empirical model of the neutron SF was developed in Ref. [15]. In Ref. [15] the neutron SF was obtained after subtraction the proton electroproduction data from corresponding deuterium data. Comparing the results of Refs. [4] and [15] in the overlap region, we observe somewhat worse agreement for F_2^n , unlike a nice agreement for F_2^p . A significant part of this disagreement arises from a different treatment of smearing with momentum distribution and the binding effect in the deuteron in Refs. [4] and [15]. In order to minimize this bias, we will model the neutron in the resonance region as follows. We calculate F_2^n for $W < 2 \text{ GeV}$ using the RES fit of F_2^p [11] and the ratio $R_{np} = F_2^n/F_2^p$ computed using the DIS fit of Ref. [3, 4]. We aim to model the neutron SF down to the $\Delta(1232)$ region and inelastic threshold. This region requires somewhat special consideration. In particular, it follows from analysis of Ref. [15] that $R_{np} \approx 1$ in the $\Delta(1232)$ region. We therefore assume equal contribution to the proton and the neutron from the $\Delta(1232)$ resonance, for which we use the notation F_2^Δ , and consider the following model for the neutron SF in the region $W < W_2$:

$$F_2^{n(\text{RES})} = R_{np} \left(F_2^{p(\text{RES})} - F_2^\Delta \right) + F_2^\Delta, \quad (7)$$

where the proton F_2^{RES} and F_2^Δ computed using the fit of Ref. [11] while the ratio R_{np} is computed using SF of the DIS fit of Ref. [4].

3. The deuteron structure function

In the region $x > 0.15$ the inelastic scattering of leptons off nuclei is dominated by incoherent scattering off bound proton and neutron. We consider the process in the target rest frame. The deuteron structure function F_2^d can be written as follows (for more detail see Ref. [6, 14]):

$$F_2^d(x, Q^2) = \int d^3\mathbf{p} |\Psi_d(\mathbf{p})|^2 K [F_2^p(x', Q^2, p^2) + F_2^n(x', Q^2, p^2)], \quad (8)$$

where we consider F_2^d as a function of $x = Q^2/(2Mq_0)$, the integration is taken over the momentum of the bound nucleon \mathbf{p} and $\Psi_d(\mathbf{p})$ is the deuteron wave function in momentum

space, which is normalized as $\int d^3\mathbf{p}|\Psi_d(\mathbf{p})|^2 = 1$. Because of energy-momentum conservation, the four-momentum of the struck proton (neutron) is $p = (M_d - \sqrt{M^2 + \mathbf{p}^2}, \mathbf{p})$, where $M_d = 2M + \varepsilon_d$ is the deuteron mass and $M = (M_p + M_n)/2$ the mass of the isoscalar nucleon and $\varepsilon_d \approx -2.2$ MeV the deuteron binding energy. We use the coordinate system in which the momentum transfer \mathbf{q} is antiparallel to the z axis, p_z and \mathbf{p}_\perp are the longitudinal and transverse component of the nucleon momentum. In this system the factor $K = (1 + \gamma p_z/M)(1 + x'^2(4p^2 + 6\mathbf{p}_\perp^2)/Q^2)/\gamma^2$, where $p^2 = p_0^2 - \mathbf{p}^2$ and $x' = Q^2/(2p \cdot q)$ are the invariant mass and the Bjorken variable of off-shell nucleon, respectively, and $\gamma^2 = 1 + 4x^2M^2/Q^2$ [6].

We verify our approach by comparing the model predictions with various measurements. Such a comparison is illustrated in Fig.1 to 2. In Fig.1 we show the predictions for the proton and the deuteron F_2 as a function of W^2 computed for a few fixed Q^2 together with the data from SLAC [16], JLab [17, 19], NMC [20], and HERMES [18] (the values of Q^2 in Fig.1 were selected such to maximize the overlap between data from different experiments). We observe a good agreement between model predictions and data in a wide region of W for both, the proton and the deuteron. Figure 2 shows the results for the ratio F_2^n/F_2^d of the neutron and the deuteron SF. The model predictions are compared with data from BoNuS experiment [1] for a few fixed values of Q^2 shown in the plots.

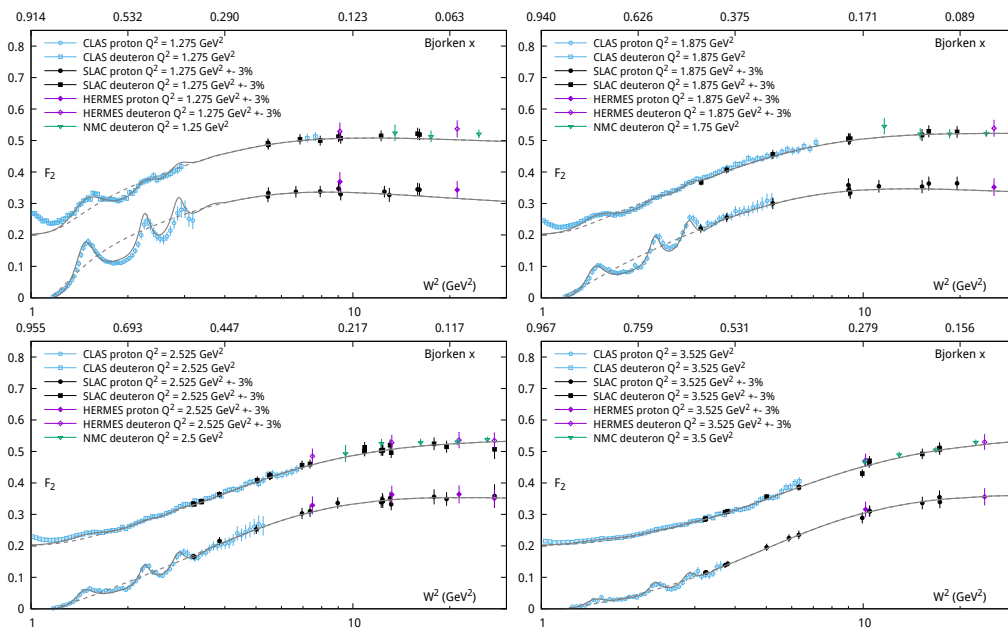


Fig. 1. (Color online) The proton and the deuteron structure functions as a function of W^2 computed at $Q^2 = 1.275, 1.875, 2.525, 3.525$ GeV 2 (the values of Bjorken x are also shown in the upper x axis). The proton data points are from SLAC [16], JLab CLAS [17], and HERMES [18] measurements, while the deuteron data are from CLAS [19], NMC [20], and HERMES [18]. The data points are selected for the given value of $Q^2 \pm 3\%$. For a better visibility the deuteron data are shifted up by 0.2. The dashed and the solid curves respectively show the predictions of the DIS and the hybrid DIS-RES model discussed in the text.

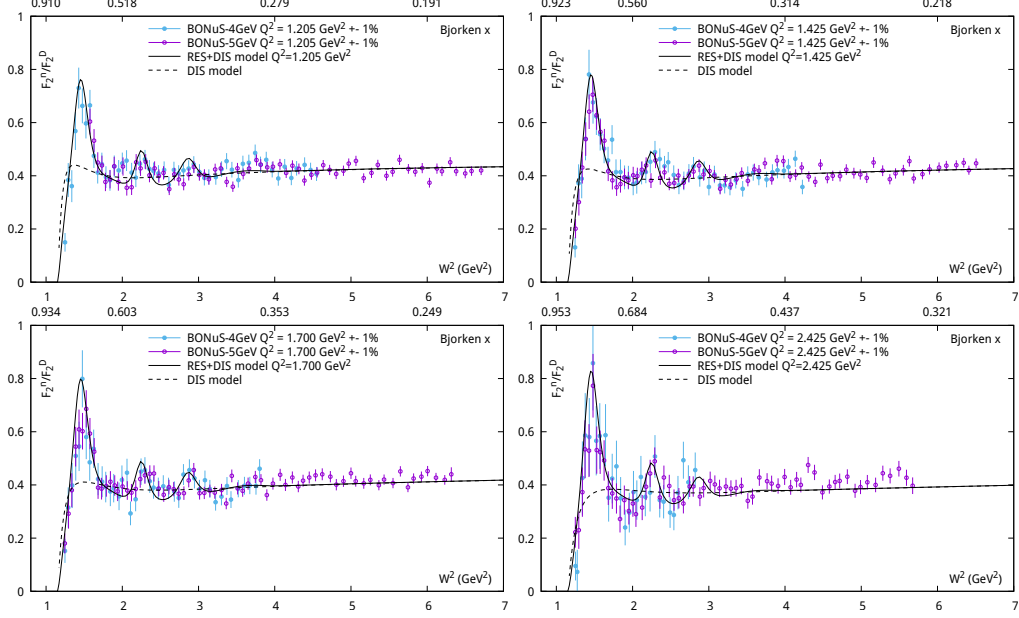


Fig. 2. (Color online) The ratio of the neutron and the deuteron structure functions F_2^n/F_2^D computed at $Q^2 = 1.205, 1.425, 1.700, 2.425 \text{ GeV}^2$ as a function of W^2 (the values of Bjorken x are also shown in the upper x axis). The data points are from the measurement by BoNuS experiment [1] at 4 GeV (closed circles) and 5 GeV (open circles) selected for the given values of $Q^2 \pm 1\%$. The dashed and the solid curves respectively show the predictions of the DIS and the hybrid DIS-RES model discussed in the text.

From this comparison we observe a good agreement of our model with data in the full region of W . We also note a good performance of the model in the $\Delta(1232)$ resonance region indicating the validity of Eq.(7) for the neutron SF.¹

A good agreement with data allows us to proceed with a detailed study of the ratio R^d which is traditionally used to measure the nuclear effects on the partonic level. We focus on the region of relatively low values of $Q^2 < 10 \text{ GeV}^2$ and large Bjorken $x > 0.1$, which span the nucleon resonance region as well as the RES-DIS transition region. The ratio $r_d = 1/R^d$ computed using the DIS as well as a hybrid DIS-RES model of Sec.2 is shown in Fig. 3. In the left panel we show r_d vs. Bjorken x for the DIS model computed at a few different Q^2 . For $x < 0.55$ we observe almost no Q^2 dependence, while the region of larger x shows a strong Q^2 dependence which is because of the target mass correction. Note that r_d has the inflection point at $x \approx 0.4$ at which $\partial_x^2 r_d = 0$. For this reason r_d is almost a linear function of x for $0.25 < x < 0.55$ with the slope $\partial_x r_d \approx 0.1$ [10]. The latter is driven by the average energy $\varepsilon = p_0 - M$ of the bound nucleon, $\langle \varepsilon \rangle = \varepsilon_d - \langle T \rangle$ with $\langle T \rangle = \langle \mathbf{p}^2 \rangle / (2M)$ the average kinetic energy, and by the average virtuality of the bound nucleon $\langle v \rangle = 2(\langle \varepsilon \rangle - \langle T \rangle) / M$ [6, 7]. We also note that the account of the nuclear binding

¹The details of the model and comparison with data will be discussed elsewhere.

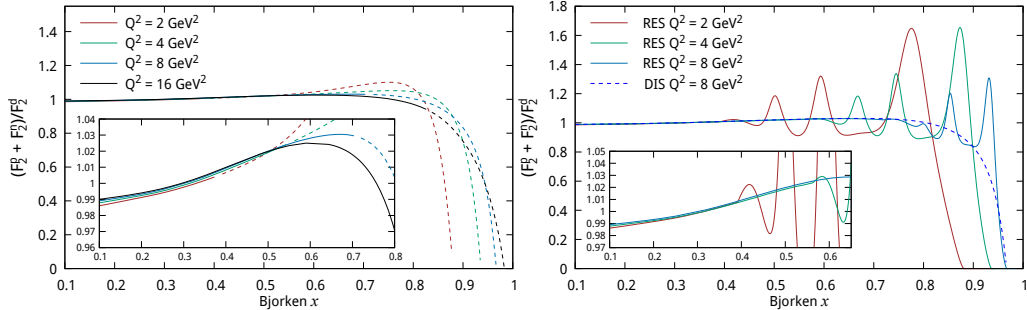


Fig. 3. (Color online) The ratio $(F_2^p + F_2^n)/F_2^d$ computed as a function of Bjorken x for $Q^2 = 2, 4, 8, 16 \text{ GeV}^2$ using the DIS model (left panel) and the combined DIS-RES model (right panel) discussed in the text. For the DIS model, the solid lines indicate the region $W > 2 \text{ GeV}$ while the dashed lines show the result from $W = 2 \text{ GeV}$ down to inelastic threshold for each value of Q^2 . The inset shows a magnified region $0.1 < x < 0.8$.

correction [21, 22] together with off-shell effect allows us to describe all available data on the nuclear EMC effect in heavy and light nuclei as discussed in detail in Refs. [6, 8, 23].

The results of our hybrid DIS-RES model are shown in the right panel of Fig. 3. For small and intermediate x values, which correspond to $W > 2 \text{ GeV}$, the behavior of r_d is identical to that of the DIS model. For larger x values, which correspond to the resonance region, r_d shows pronounced oscillations with the peaks' amplitude and position to be strongly dependent on Q^2 . For example, at $Q^2 = 2 \text{ GeV}^2$ the nuclear corrections can be as much as 60% in the Δ resonance region and reach about 30% and 15% in the second and third resonance region, respectively. As Q^2 is rising the resonance curve approaches a smooth DIS curve, however even at $Q^2 = 8 \text{ GeV}^2$ significant oscillations are present in the $\Delta(1232)$ region as well as in the second resonance region.

We consider r_d instead of traditional R^d in order to facilitate discussion at large values of Bjorken x , as $r_d \rightarrow 0$ at the pion production threshold. In this context we would like to emphasize that the behavior of $F_2^{p,n}$ near the inelastic threshold has a strong impact on r_d that allows us to test different models. In particular, TMC of Ref. [5] violates the threshold behavior, as was discussed in Sec.2, and using Eq.(2) for the proton and neutron SF in Eq.(8) for low $Q^2 < 5 \text{ GeV}^2$ would lead to unphysical values of $r_d > 1$ at large x near the inelastic threshold. We recall that the factor $f_{\text{th}}(W)$ ensures F_2^{DIS} to vanish on the inelastic threshold and also has a significant impact on r_d in the region of large Bjorken x . We also remark that the model of Ref. [11] respects the threshold behavior resulting in vanishing F_2^{RES} at the inelastic threshold.

We now compare in more detail the model predictions with recent data of BoNuS experiment on r_d [2] and F_2^n/F_2^d [1]. The left panel of Fig. 4 shows the data points from the measurement of Ref. [2]. The dashed line connects the points obtained with the DIS model using Eq.(8) computed at the central values of each x -bin with the corresponding average Q^2 . The other lines show the predictions in our combined DIS-RES model using different assumptions about kinematics of the data points. In particular, the dotted line is the result computed at the central values of each x -bin with the corresponding average Q^2 , similar to the DIS case (dashed line). We observe the strong oscillation of r_d for $x > 0.4$

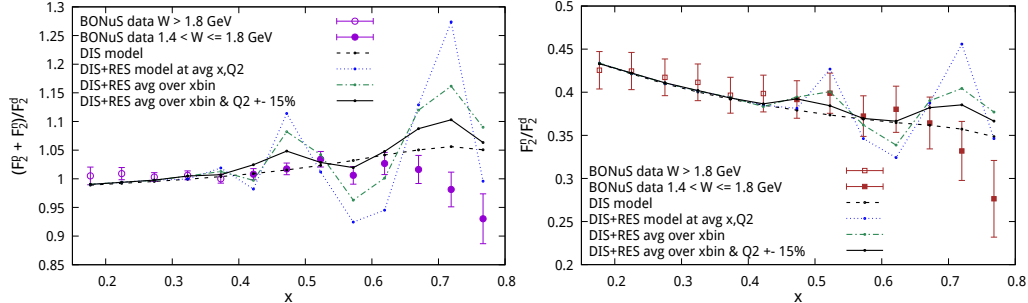


Fig. 4. (Color online) Left panel: data points on the ratio $(F_2^p + F_2^n)/F_2^d$ from BoNuS experiment [2] together with the result of analysis described in the text. Right panel: data points on the ratio F_2^n/F_2^d from BoNuS experiment [1] together with the result of analysis described in the text. Solid symbols indicate the region of $W < 1.8$ GeV while open symbols correspond to the DIS region $W > 1.8$ GeV.

with rising amplitude which is due to the resonance behavior of the underlying nucleon SF. These oscillations smooth out if we integrate (average) the structure functions over the x -bin (dashed-dotted line). Further smoothing of the resonance behavior is observed if, in addition to the x -bin averaging, we average over Q^2 . The solid line is the result of such averaging assuming a uniform Q^2 distribution for each of the data point around its central value within $\pm 15\%$. The right panel of Fig. 4 shows the data points on the ratio F_2^n/F_2^d as measured by the BoNuS experiment [1] together with the result of similar analysis.

In summary, we discussed a hybrid DIS-RES model for the proton and neutron SF basing ourselves on the results of two independent fits, respectively, in the DIS and the resonance region. The model was applied to compute the deuteron SF in the kinematic domain typical for JLab experiments with particular emphasis on the region $W < 3$ GeV. We found good agreement with BoNuS data on the ratios F_2^n/F_2^d and $(F_2^p + F_2^n)/F_2^d$ for $W > 1.8$ GeV. For smaller W these ratios are subject to strong oscillations due to resonance behavior of the nucleon SF. The averaging over x and Q^2 smooth out the resonance oscillations making the result close, but not identical, to the prediction of the DIS model. A more detailed comparison with BoNuS data at very large x would require further analysis.

I am grateful to S.Alekhin, V.Barinov and R.Petti for useful discussions and M.Osipenko for providing CLAS structure function data. The work was partially supported by the grant of the Russian Science Foundation No.14-22-00161.

REFERENCES

1. Tkachenko S. et al. [CLAS Collaboration] Measurement of the structure function of the nearly free neutron using spectator tagging in inelastic $^2\text{H}(e, e'p)\text{X}$ scattering with CLAS // *Phys. Rev.C.* — 2014. — V. 89. — P. 045206. — arXiv:1402.2477 [nucl-ex].

2. *Griffioen K.A., Arrington J., Christy M.E., Ent R., Kalantarians N., Keppel C.E., Kuhn S.E., Melnitchouk W., Niculescu G., Niculescu I., Tkachenko S., Zhang J.* Measurement of the EMC Effect in the Deuteron // *Phys. Rev.C.* — 2015. — V. 92, no. 1. — P. 015211. — arXiv:1506.00871.
3. *Alekhin S., Melnikov K., Petriello F.* Fixed target Drell-Yan data and NNLO QCD fits of parton distribution functions // *Phys. Rev.D.* — 2006. — V. 74. — P. 054033. — arXiv:hep-ph/0606237.
4. *Alekhin S., Kulagin S.A., Petti R.* Modeling lepton-nucleon inelastic scattering from high to low momentum transfer // *AIP Conf. Proc.* — 2007. — V. 967. — P. 215–224. — arXiv:0710.0124 [hep-ph].
5. *Georgi H., Politzer H.D.* Freedom at Moderate Energies: Masses in Color Dynamics // *Phys. Rev.D.* — 1976. — V. 14. — P. 1829.
6. *Kulagin S.A., Petti R.* Global study of nuclear structure functions // *Nucl. Phys.A.* — 2006. — V. 765. — P. 126–187. — arXiv:hep-ph/0412425.
7. *Kulagin S.A., Piller G., Weise W.* Shadowing, binding and off-shell effects in nuclear deep inelastic scattering // *Phys. Rev.C.* — 1994. — V. 50. — P. 1154–1169. — arXiv:nucl-th/9402015.
8. *Kulagin S.A., Petti R.* Structure functions for light nuclei // *Phys. Rev.C.* — 2010. — V. 82. — P. 054614. — arXiv:1004.3062 [hep-ph].
9. *Kulagin S.A., Petti R.* Nuclear parton distributions and the Drell-Yan process // *Phys. Rev.C.* — 2014. — V. 90, no. 4. — P. 045204. — arXiv:1405.2529 [hep-ph].
10. *Alekhin S.I., Kulagin S.A., Petti R.* Nuclear Effects in the Deuteron and Constraints on the d/u Ratio // *Phys. Rev.D.* — 2017. — V. 96, no. 5. — P. 054005. — arXiv:1704.00204.
11. *Christy M.E., Bosted P.E.* Empirical fit to precision inclusive electron-proton cross-sections in the resonance region // *Phys. Rev.C.* — 2010. — V. 81. — P. 055213. — arXiv:0712.3731 [hep-ph].
12. *Bloom E.D., Gilman F.J.* Scaling, duality, and the behavior of resonances in inelastic electron-proton scattering // *Phys. Rev. Lett.* — 1970. — V. 25. — P. 1140.
13. *Melnitchouk W., Ent R., Keppel C.* Quark-hadron duality in electron scattering // *Phys. Rept.* — 2005. — V. 406. — P. 127–301. — arXiv:hep-ph/0501217.
14. *Alekhin S.I., Kulagin S.A., Liuti S.* Isospin dependence of power corrections in deep inelastic scattering // *Phys. Rev.D.* — 2004. — V. 69. — P. 114009. — arXiv:hep-ph/0304210.
15. *Bosted P.E., Christy M.E.* Empirical fit to inelastic electron-deuteron and electron-neutron resonance region transverse cross-sections // *Phys. Rev.C.* — 2008. — V. 77. — P. 065206. — arXiv:0711.0159 [hep-ph].

16. *Whitlow L.W., Riordan E.M., Dasu S., Rock S., Bodek A.* Precise measurements of the proton and deuteron structure functions from a global analysis of the SLAC deep inelastic electron scattering cross-sections // *Phys. Lett.B.* — 1992. — V. 282. — P. 475–482.
17. *Osipenko M. et al.* [CLAS Collaboration] A Kinematically complete measurement of the proton structure function F_2 in the resonance region and evaluation of its moments // *Phys. Rev.D.* — 2003. — V. 67. — P. 092001. — arXiv:hep-ph/0301204.
18. *Airapetian A. et al.* [HERMES Collaboration] Inclusive Measurements of Inelastic Electron and Positron Scattering from Unpolarized Hydrogen and Deuterium Targets // *JHEP.* — 2011. — V. 05. — P. 126. — arXiv:1103.5704 [hep-ex].
19. *Osipenko M. et al.* [CLAS Collaboration] Measurement of the deuteron structure function F_2 in the resonance region and evaluation of its moments // *Phys. Rev.C.* — 2006. — V. 73. — P. 045205. — arXiv:hep-ex/0506004.
20. *Arneodo M. et al.* [New Muon Collaboration] Measurement of the proton and deuteron structure functions, F_2^p and F_2^d , and of the ratio σ_L/σ_T // *Nucl. Phys.B.* — 1997. — V. 483. — P. 3–43. — arXiv:hep-ph/9610231.
21. *Akulinichev S.V., Kulagin S.A., Vagradov G.M.* The Role of Nuclear Binding in Deep Inelastic Lepton Nucleon Scattering // *Phys. Lett.B.* — 1985. — V. 158. — P. 485–488.
22. *Kulagin S.A.* Deep Inelastic Scattering on Nuclei: Impulse Approximation and Mesonic Corrections // *Nucl. Phys.A.* — 1989. — V. 500. — P. 653–668.
23. *Kulagin S.A.* Nuclear Parton Distributions // *EPJ Web Conf.* — 2017. — V. 138. — P. 01006. — arXiv:1612.07741.